REVIEW

Cross Tropopause Transport of Water by Mid-Latitude Deep Convective Storms: A Review

Pao K. Wang[1, *], Shih-Hao Su[1, 2], Zdeněk Charvát[3], Jindřich Šťástka[3], and Hsin-Mu Lin[4]

[1] *Department of Atmospheric and Oceanic Sciences, University of Wisconsin-Madison, Madison, USA*
[2] *Department of Atmospheric Science, National Taiwan University, Taipei, Taiwan*
[3] *CHMI - Satellite Department, Praha, Czech Republic*
[4] *Environmental Modeling Center, NCEP/NOAA, Camp Springs, Maryland, USA*

ABSTRACT

Recent observational and numerical modeling studies of the mechanisms which transport moisture to the stratosphere by deep convective storms at mid-latitudes are reviewed. Observational evidence of the cross-tropopause transport of moisture by thunderstorms includes satellite, aircraft and ground-based data. The primary satellite evidence is taken from both conventional satellite of thunderstorm images and CloudSat vertical cloud cross-section images. The conventional satellite images show cirrus plumes above the anvil tops of some of the convective storms where the anvils are already at the tropopause level. The CloudSat image shows an indication of penetration of cirrus plume into the stratosphere. The aircraft observations consist of earlier observations of the "jumping cirrus" phenomenon reported by Fujita and recent detection of ice particles in the stratospheric air associated with deep convective storms. The ground-based observations are video camera records of the jumping cirrus phenomenon occurring at the top of thunderstorm cells. Numerical model studies of the penetrative deep convective storms were performed utilizing a three-dimensional cloud dynamical model to simulate a typical severe storm which occurred in the US Midwest region on 2 August 1981. Model results indicate two physical mechanisms that cause water to be injected into the stratosphere from the storm: (1) the jumping cirrus mechanism which is caused by the gravity wave breaking at the cloud top, and (2) an instability caused by turbulent mixing in the outer shell of the overshooting dome. Implications of the penetrative convection on global processes and a brief future outlook are discussed.

1. INTRODUCTION

Water plays many important roles in the atmosphere. The most familiar is the formation of clouds and precipitation that are of central importance to traditional weather science. But water also plays an important role in the chemistry of the atmosphere. Aside from reactions in the troposphere, water vapor is also involved in significant stratospheric chemical processes as well (Brasseur et al. 1999). For example, it is the main source material for making the ozone-depleting HO_x radicals and the condensed form of water substance serves as a catalytic surface for heterogeneous reactions involving NO_x and halogen species in the polar stratospheric clouds (Solomon 1999).

Water substance also plays an important role in the global climate process. Water vapor is responsible for most of the greenhouse warming of the Earth's atmosphere (see, e.g., Liou 1992). Although the absolute majority of water vapor resides in the troposphere, the small amount of water vapor in the stratosphere may have very strong climatic impact. Stratospheric water vapor shows both seasonal variations and Northern-Southern hemispheric asymmetry (Pan

---
* *Corresponding author*
  E-mail: pao@windy.aos.wisc.edu

et al. 1997, 2000). Reliable long term climate forecasts require accurate descriptions of the response of stratospheric water vapor to climate forcing (Shindell 2001; Forster and Shine 2002). Since its residence time can be more than a year, the fluctuation of stratospheric water vapor can be an important climate forcing itself. Frostpoint hygrometer measurements of water vapor in the lower stratosphere (LS) show that the LS vapor concentration had been increasing at ~1% per year for at least two decades persistently up to about the year 2000 (Oltmans et al. 2000; Rosenlof et al. 2001) and has been decreasing since then (Solomon et al. 2007). This time-dependent behavior of the stratospheric water vapor concentration and its potential influence on the global climate needs to be assessed carefully.

Currently, three pathways are thought to be responsible for the presence of water vapor in the stratosphere: (1) slow large scale ascent carrying moisture gradually from the lower troposphere to the upper troposphere and eventually passing through the region of coldest temperatures in the tropical tropopause layer into stratosphere; (2) rapid convective transport of moisture from the troposphere, presumably by the strong updrafts of deep convective storms that carry both ice particles and water vapor into the stratosphere; and (3) oxidation of upper stratospheric methane (CH_4) to form water vapor coupled with subsequent downward transport. It is also possible to have a two-stage process, where convection lofting parcels and ice rise to the upper troposphere, followed by gradual dehydration as the parcels ascend into the stratosphere (Rosenlof 2003). The 3rd pathway has been considered as insignificant in the lower stratosphere (e.g., Rosenlof 2003; Myhre et al. 2007). This leaves either the first or the second pathway and no definite conclusion has been reached as to which is the major pathway for water to rise into the stratosphere . There are considerable debates about the relative importance of the two, but recently evidence is mounting showing that convective penetration actually occurs more frequently than previously thought and hence may represent the major pathway via which water vapor enters the stratosphere.

Previous studies of the entry pathways of stratospheric water focused almost exclusively on the tropics and the main motivation was to determine the dehydration mechanism to explain the dryness of the stratosphere. But deep convection occurs in both low and middle latitudes and transports water to the stratosphere. This transport occurs in the tropics, it may also occur in the mid-latitudes as our recent studies clearly show that this is the case. In order to explain the global hydrological cycle including the stratosphere, in our opinion, the mid-latitude convective transport should also be included. This paper will summarize some recent observational and modeling studies on the convective transport of water vapor in the mid-latitudes. Brief discussions of the tropical deep convective transport of water will also be included for obtaining a global perspective.

2. SATELLITE OBSERVATIONS OF THE CROSS-TROPOPAUSE CONVECTIVE TRANSPORT OF WATER SUBSTANCE

The primary evidence of the cross-tropopause convective transport of water substance has been provided by satellite observations. Past studies on this topic have shown two possible approaches using satellite observations to demonstrate such transport mechanism. The first approach described by Setvák and Doswell (1991) and Levizzani and Setvák (1996) is based on the observations of plume-like features on the tops of some of the convective storms. The second approach utilizes the brightness temperature difference between water vapor absorption and infrared window bands (e.g., Fritz and Laszlo 1993; Setvák et al. 2008).

The first observational report specifically related to the deep convective cross-tropopause transport of water substance was the satellite observation made by Setvák and Doswell (1991). They found that in some cases, chimney plume-like features appear on the tops of the storm anvils. If the sun angle is low (as in the case of either early morning or later afternoon), the plume often casts clear shadow on the anvil. It is also possible to have more than one plume appear above the anvil.

Figure 1 shows an example of the above-anvil plume (Setvák 2004, personal communication). This was a severe tornadic storm system which occurred over the Ibiza Island of the Balearic Islands, Spain. The plume is seen starting out from a point very near the overshooting top of the storm and stretching and widening downwind in a NE direction. The plume casts a shadow on top of the anvil. In fact, the other storm to the west (left) of this one also has an above anvil plume, although it appears to be less intense.

Figure 2 shows another example of such plumes. In this case, the satellite is viewing the storm at nearly nadiral direction and the sun angel is relatively high, hence the shadow is not as obvious but nevertheless can still be discerned along the north rim of the plume.

The plumes can usually be seen in the visible and near-infrared (NIR) channels; hence they should consist of ice particles given the very low temperature at such a high level (usually -50 to -60°C). For this reason, they are sometimes called by others stratospheric cirrus plumes or simply stratospheric cirrus (e.g., Fujita 1982). More precisely they should be referred to as above-anvil ice-plumes. Sometimes, they can also be seen in thermal infrared images, depending on their height and the temperature profile of the lower stratosphere. The fact that satellite images show that the plumes usually have high 3.7 - 3.9 m reflectivity implies that the ice particles in the plume must be quite small, possibly of the order of several μm (Levizzani and Setvák 1996).

Initially thought to be a rare phenomenon, the anvil top plumes are now known to occur regularly above convective storms in many parts of the world. Figure 3 shows an image taken by MODIS instrument on Aqua satellite which shows

a series of thunderstorms occurring over northern Mexico. Almost every well-developed storm cell in this image has an anvil top plume.

The size of the plumes varies greatly. Some are very wide and extend downwind to a length longer than the storm anvil while others may be very short and narrow. Levizzani and Setvák (1996) investigated more examples of anvil top plumes and estimated that most of them are 1 - 3 km above the anvil. If the anvil top is already at the tropopause, then these plumes must be in the lower stratosphere.

The plume examples shown previously require the presence of condensed phase such as ice. It is also possible

Fig. 3. MODIS Aqua band 1 image of a storm system in north Mexico at 2005 UTC 07 May 2007, showing multiple extensive above anvil plumes (Courtesy of Martin Setvák, data source: NASA/LAADS).
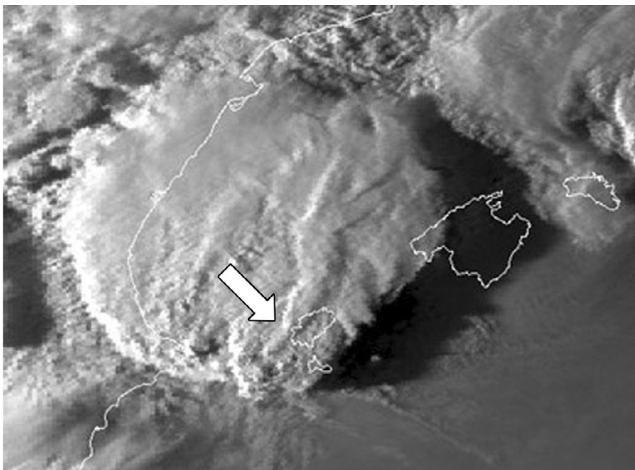

Fig. 1. NOAA-12 AVHRR band 1 image at 1724 UTC 11 September 1996, of a severe tornadic storm system occurring over the Ibiza Island of the Balearic Islands of Spain (39º30'N3º00'E). The plume is indicated by the white arrow (Courtesy of Martin Setvák, data source: NOAA/CHMI).

that the plume consists of purely water vapor without any condensed phase, and hence cannot be seen by visible band. A method developed in the 1990s (Fritz and Laszlo 1993) of observing the convective vertical transport of water vapor through the tropopause is based on the brightness temperature difference (BTD) between the water vapor and infrared window bands as mentioned above. The BTD is typically negative for lower clouds and cloud-free areas, since the water vapor band radiance is usually lower than infrared window band radiance. However, positive BTD values appear above cloud tops of most of convective storms. This can be explained by the presence of LS moisture in the case of a temperature inversion above the tropopause. The BTD field is often well correlated with the coldest pixels in the infrared window band. However, in some cases these two fields are not quite correlated. Such a case was described by Setvák et al (2008) who offered an explanation that the effect may be caused by local moistening of the air above the storm by the storm itself, i.e., an above-anvil vapor plume. Another possible explanation of the low correlation is due to the emissivity/scattering effects within the cloud and is recently a subject of further studies. Figure 4 shows example of the case discussed by Setvák et al (2008).

3. CLOUD MODEL SIMULATION OF CROSS-TROPOPAUSE TRANSPORT OF WATER SUBSTANCE

The above-anvil plume phenomenon in the lower stratosphere poses an interesting question, where does the water come from? One possibility is that the plume forms from water vapor that is already in the stratosphere and by the storm's motion; for example, the wave motion induced by
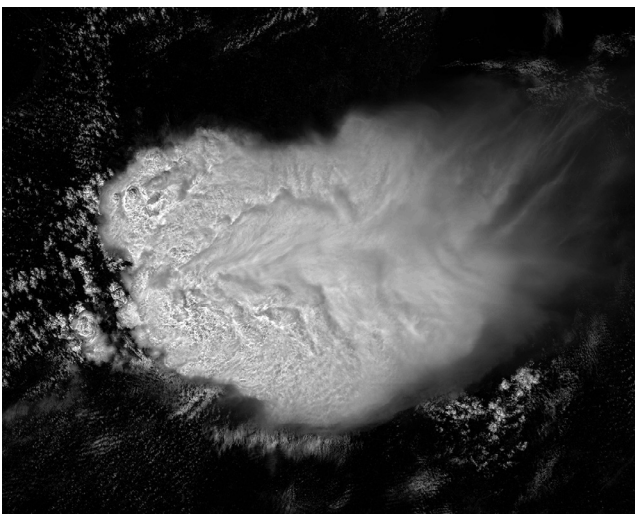

Fig. 2. MODIS Aqua band 1 image of an intense storm system over northern Illinois, US, at 1855 UTC 13 July 2004, showing an extensive plume above the anvil of the storm (data source: NASA/LAADS).
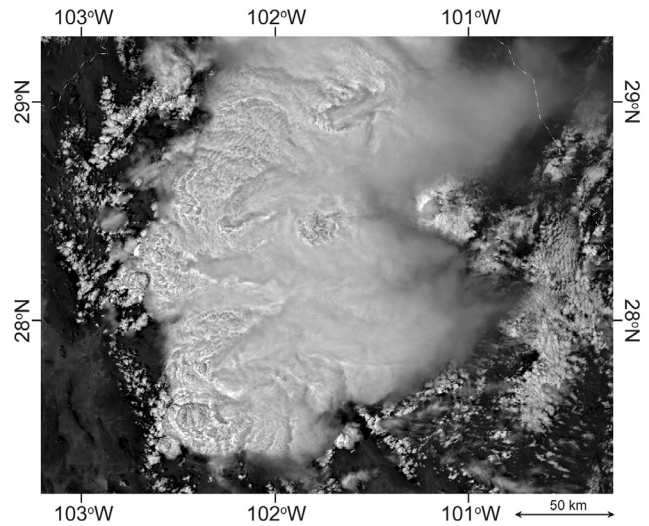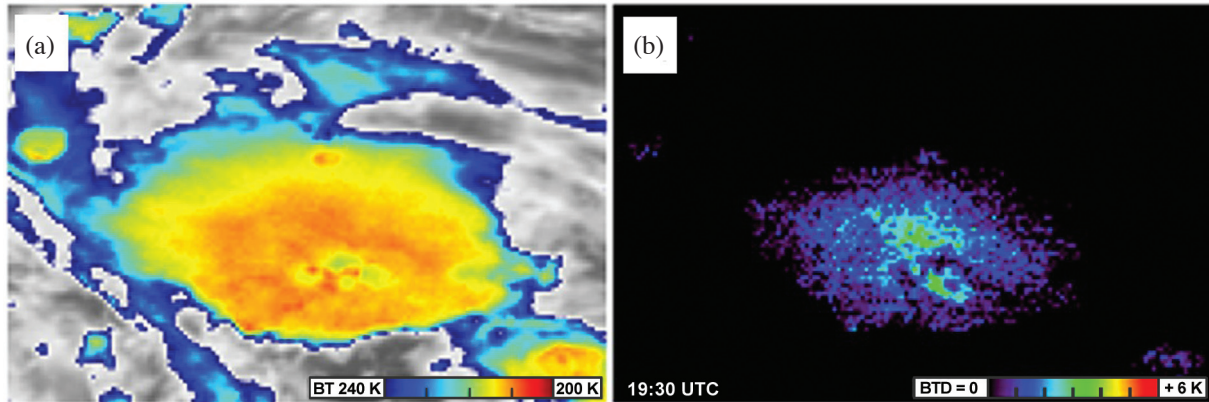
Fig. 4. Meteosat 8 (MSG-1) SEVIRI image at 1930 UTC 28 June 2005. Left IR 10.8 μm band with color enhanced brightness temperature range 200 - 240 K. BTD (6.2 - 10.8 μm) images on the right (from Setvák et al. 2008).

the intense updraft, that causes the air to be lifted and cooled adiabatically to form cirrus clouds, much like the formation of pileus cloud is often observed above the overshooting dome of convective storms. Both the observed plume morphology and the results of numerical cloud model simulations with a humid layer in the stratosphere above the storm indicate that this is unlikely the case.

Another more likely possibility is that the plume derives the water from the thunderstorm itself, that is, the storm ejects either ice particles upward directly into the lower stratosphere or it injects water vapor into the stratosphere which is subsequently nucleated in situ to form the cirrus plume, or the combination of both. In either case, the source of water substance for the plume is the troposphere and the formation of the cirrus plume implies a cross-tropopause transport of water substance.

This possibility was first investigated by Wang (2003) who used a 3-D nonhydrostatic cloud model WISCDYMM (Wisconsin Dynamical/Microphysical Model, see Straka 1989; Johnson et al. 1993, 1994; Wang 2007) to simulate a typical US High Plains severe thunderstorm to see if the plume phenomenon occurs in the simulated storm. This storm occurred on 2 August 1981 in the upper Midwest of the US which was observed intensely by the Cooperative Convective Precipitation Experiment (CCOPE) field campaign and will be referred to heretofore as the CCOPE supercell. The sounding used to initialize this storm and the observational aspects of this supercell have been given by Knight (1982) and Wade (1982). It also has been simulated numerically using the same cloud model by Johnson et al. (1993, 1994) and Lin et al. (2005). The resolution adopted by Wang (2003) was $1 \times 1 \times 0.2$ km³ which was higher than the one performed by Johnson et al. (1993, 1994) who used the same horizontal resolution but the vertical resolution was 0.5 km. However, the major features of the plumes are very similar in these cases, indicating that the plume process is relatively insensitive to model resolution.

The simulation by Wang (2003) demonstrates that thunderstorms can perform the cross-tropopause transport of water substance via the gravity wave breaking at the storm top and provide the source material for the formation of the above-anvil ice plumes. The two figures below, Figs. 5 and 6, are taken from a new simulation similar to Wang (2003) but with a higher resolution of $0.5 \times 0.5 \times 0.2$ km³. Again, the major features are very similar to that in Wang (2003) although the finer resolution simulation usually results in a somewhat more vigorous storm with greater maximum updraft and slightly higher plume levels. Also, the timing of the wave breaking and other related events may also change slightly with different resolution, but the overall sequences of the dynamical processes are still quite similar.

It is worth noting that the choice of this storm for the simulation is quite arbitrary and simply due to its qualification as an intense thunderstorm. We have simulated other intense thunderstorms and many of them show the same plume-generation phenomenon. While the CCOPE storm is a supercell, there are also many simulated multicell storms (such as the one occurred in southern Germany on 5 August 2003 and will be discussed at the end of section 4) that produce plumes.

Figure 5 shows a few snapshots of the central vertical east-west cross-section of the simulated CCOPE storm. It is divided into the left panel and right panel, each representing a different plume formation mechanism. The left panel shows the jumping cirrus plume formation. The right panel shows the overshooting plume formation. The color shades show the RHi (relative humidity with respect to ice) field and black contours represent the equivalent potential temperature θ_e. The RHi field is more useful for comparing the simulated plume phenomenon with direct observations as the relative humidity is more closely linked to condensation and hence the visible features of the plume. The θ_e field, on the other hand, is better in showing the dynamical process as the variable θ_e has included the thermal, pressure and
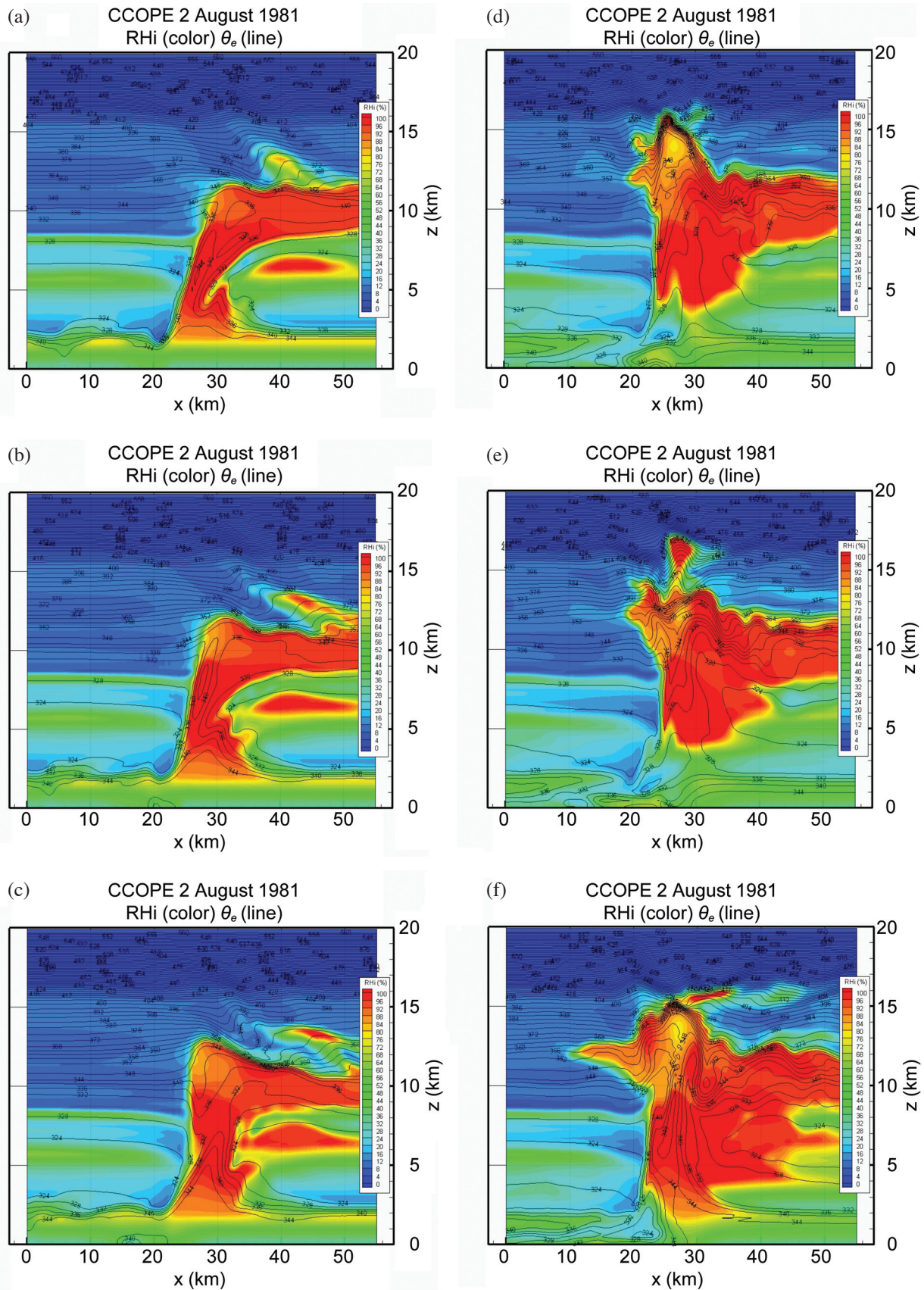
Fig. 5. Snapshots of the RHi and θ_e fields in the central vertical cross-section of the storm. Left panel: (a) t = 22 min, (b) t = 26 min, (c) t = 30 min. Right panel: (d) t = 92 min, (e) t = 96 min, (f) t = 120 min. Upper level winds are westerly (winds from left to right).

Fig. 6. Snapshots of the water vapor mixing ratio (q_v) and θ_e fields in the central vertical cross-section of the storm. Left panel: (a) t = 24 min, (b) t = 28 min, (c) t = 32 min. Right panel: (d) t = 92 min, (e) t = 96 min, (f) t = 120 min. Upper level winds are westerly (winds from left to right).

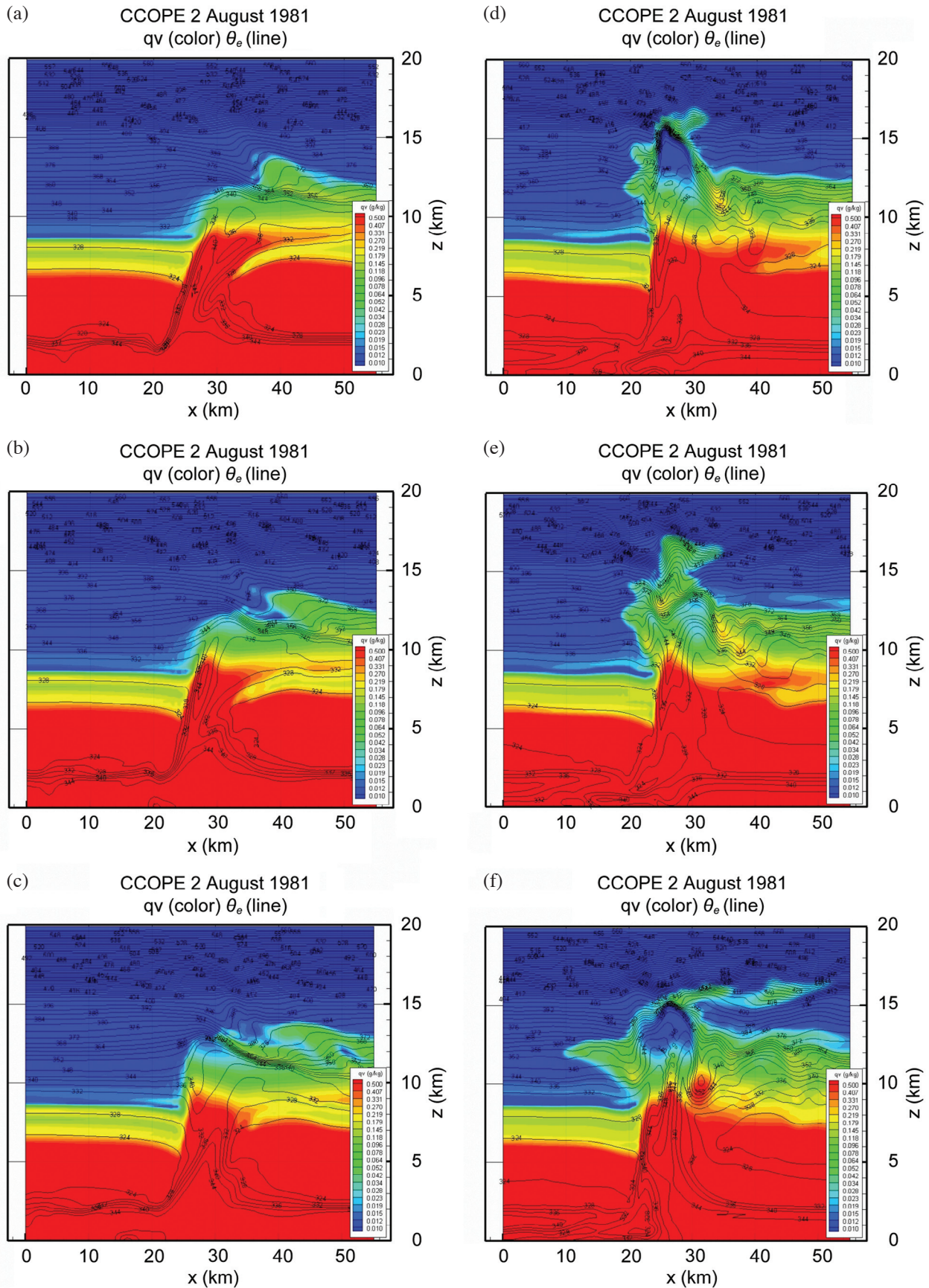moisture effect in itself and its distribution serves as a basis for distinguishing adiabatic and diabatic processes.

3.1 Jumping Cirrus Plume Formation (Fig. 5, Left Panel)

The jumping cirrus phenomenon occurs soon after the first time the overshooting dome forms. After the dome reaches z ~13 km at t = 16 min (not shown here), it starts to go downward as in an oscillation. We see that at t = 22 min (a), the overshooting top of the storm has dropped to ~12 km. At the same time, gravity waves propagate upward and downstream. At the cloud top at x ~45 km, the anvil is going through a wave breaking process. The anvil sheet is bulging up and pointing to the upstream. The wave breaking is clearly demonstrated by the shape of those θ_e contours associated with the bulge. They curl over in a manner similar to the breaking of water waves when they move close to the shore. Water vapor is seen penetrating the θ_e contours, indicating that the wave breaking is a non-adiabatic process. At t = 26 min, the broken wave takes the shape of a cloud jumping upward whose "front" reaches an altitude of ~15 km. This is the "jumping cirrus" as observed by Fujita (1982, 1989) and more detail will be given in section 4. We see that part of this jumping cirrus has completely been separated from the anvil.

As time goes on, as in Fig. 5c at t = 30 min, the whole jumping cirrus is separated from the anvil and eventually takes the shape of an above-anvil ice plume. Since the plume forms from downwind of the overshooting area, it usually does not reach the overshooting dome. It is possible that many anvil top plumes that seem to originate far from the overshooting top may form by this process. From the thunderstorm cases we have simulated, the jumping cirrus plumes typically occur along the central line of the anvil.

3.2 Overshooting Plumes (Fig. 5, Right Panel)

The right panel of Figs. 5d - f shows the formation of overshooting plumes. The name reflects the location of the plume occurrence as it obviously comes from the overshooting area. Figure 5d shows the central cross-section of the storm at t = 92 min. At this time, the storm has already developed into a quasi-steady state supercell, with prominent overshooting top reaching ~16.5 km. It is seen that the θ_e contours are highly congested indicting very large vertical θ_e gradient ($\partial\theta_e/\partial z$). The high gradient usually indicates the high tendency to become unstable as turbulent mixing with environmental air can result in negative $\partial\theta_e/\partial z$ and hence instability. Before this time, there were already some smaller scale instabilities occurring around the overshooting top, causing some ejection of cloud mass into the stratosphere.

But at t = 96 min (Fig. 5e) the overshooting dome completely collapses, causing a very large ejection of cloud mass

into the stratosphere to an altitude as high as 17 km. Since the model has a gradual Rayleigh damping layer from 17 to 20 km, one might expect that the maximum height of the ejection may have been influenced somewhat by the damping. A sensitivity run with the domain ceiling at z = 30 km showed that the highest elevation reached by the plume is also about 17 km, indicating that the damping effect is insignificant. The overall features of the wave breaking of the high-ceiling run are also quite similar to case presented here, so it appears that the wave breaking process is not sensitive to the damping height also. The anvil becomes highly wavy at this time. Since there is wind at this level, the ejection of the cloud mass is probably due to a combination of the instability and wave motion, somewhat akin to a small scale wave breaking.

The overshooting dome soon recovers as unstable boundary layer air parcels continue to rise to the tropopause and the dome continues to eject moisture into the stratosphere which eventually becomes chimney plume shaped cirrus by the action of upper level winds (Fig. 5f). This type of plume usually forms either above the downwind side or in the downstream area but in close proximity of the overshooting top.

It is worth noting that the interior of the overshooting dome is relatively dry as indicated by the low RHi, in agreement with the observation by Roach (1967). This is due to the rapid formation of ice crystals here because of the low temperatures caused by the rapid adiabatic expansion. The air in the core region of the overshooting dome largely comes from the moist boundary layer air parcels which ascend to the upper troposphere almost undiluted, causing the very cold temperature. Some thermodynamic processes related to the overshooting top are discussed by Wang (2007).

Figure 5 uses the RHi profile to represent the storm body since the high RHi region (red color, 80 - 90%) gives a good approximation of the visible storm and plume boundary and is useful for comparing with visual observations. But RHi does not represent the actual amount of water vapor since it is a function of both vapor concentration and temperature. Instead, water vapor mixing ratio q_v is a better representation of the actual vapor amount and this is shown in Fig. 6. The time of the snapshot corresponds exactly to that in Fig. 5. The color scale of q_v is designed to emphasize the cloud top region where the vapor concentration is small. Figure 6 shows that the cross-tropopause transport of water vapor is real and not an artifact due to temperature effect.

Figure 6 shows that the distribution of q_v is similar to that of RHi but with some differences. The q_v-distribution tends to be more continuous, as can be seen by comparing Figs. 6b, c with Figs. 5b and c. This is mainly because q_v is only controlled by the dynamic process of transport but not by temperature whereas RHi is controlled by both. Thus, even if the q_v distribution is uniform over a certain region, the RHi distribution can become discontinuous if the

temperature is not uniform inside the region. Figures 6d and f show very clearly that the inner core of the overshooting dome is indeed very dry and hence it is unlikely to be the source of water vapor that is injected into the stratosphere. This also has been argued by Roach (1967) who suggested that the vapor source should come from the thin shell of the overshooting dome itself instead of the core of the dome. Our preliminary trajectory analysis of air parcel suggests that the air that gets injected into the stratosphere during a severe storm like this comes largely from the upper troposphere that gets entrained into the overshooting shell. A recent cloud model study on the tropical tropopause layer (TTL) by Hassim and Lane (2010) also suggests that the plumes occurring in tropical deep convection are mainly of TTL origin, thus corroborating with the mid-latitude results obtained here.

4. JUMPING CIRRUS

The jumping cirrus phenomenon mentioned above was reported in the 1980's by Fujita (1982, 1989) but was met with much doubt, possibly due to the difficult observational conditions immediately above a severe storm and the lack of explanation on its dynamics. Fujita (1982) stated that

"One of the most striking features seen repeatedly above the anvil top is the formation of a cirrus cloud which jumps upward from behind the overshooting dome as it collapses violently into the anvil cloud."

This statement implies that the cloud not only jumped upward but was also directed upstream which, at the time, was difficult to understand. Normally we would expect the motion of a cloud to follow the direction of the wind instead of against it. For example, the storm as shown in Fig. 5 indeed tilts to the right precisely because of the upper level wind is from left to right. Now in light of what we described above, it is clear that the jumping cirrus is precisely the manifestation of the storm top gravity wave breaking process.

The modeled jumping cirrus sequence is best illustrated by Fig. 7 which is taken from Wang (2004). This figure is similar to Fig. 5 except it focuses on the jumping cirrus phenomenon and only the cloud top region of the storm is shown in each panel. It shows a series of 12 snapshots of the RHi profiles in the central east-west vertical cross-section (y = 27 km) of the simulated storm every 120 s from t = 1320 to 2640 s. Note that the vertical scale is stretched in these views. The following descriptions are condensed from Wang (2004) where more detailed descriptions can be obtained.

At t = 1320 s, the overshooting is not yet well developed and the highest point of the cloud is only slightly higher than the tropopause at 12.5 km. However, the wavy nature of the storm top is already obvious. At t = 1440 s, a cloudy patch starts to emanate from the bulge in the cloud top below. This patch is the precursor that eventually develops into a full-fledged jumping cirrus. The white arrow pointing at x ~34 km indicates the approximate position of the left (west) edge of the patch. At the same time, the overshooting top subsides, changing from a height of ~13 km to ~12.5 km, a drop of ~500 m. This seems to correspond to what Fujita (1982) described as the "collapse of the overshooting dome." While the overshooting top is subsiding, the wave crest located at x ~40 km starts to bulge up and tilt upstream. At 1560 s, a "jumping cirrus" in the form of a cirrus tongue has developed with its front edge located at x ~32 km and reaching an altitude of ~15 km. The cirrus tongue is already located higher than the overshooting top and is moving upstream.

As time goes on, the cirrus reaches further west and higher altitude as can be seen by the locations of the white arrows at the front edge. Since the altitudes of the jumping cirrus are both ~15 km at 1560 and 1680 s, the maximum altitude probably occurred somewhere in between these two times. This upstream and upward motion corresponds to what Fujita described as the "cirrus cloud which jumps upward from behind the overshooting dome." This ascending sequence of the jumping cirrus lasts about 6 min within which the cirrus rises from z ~12 to ~15 km.

Figure 8 shows the time evolution of the (x, z) position of the jumping cirrus during the "jump" stage from which the velocity components (u, w) can be obtained. The average vertical speed of the jump is therefore about 8 m s⁻¹ but the maximum vertical speed exceeds 10 m s⁻¹, and certainly is justified to be described as "jumping." The development of the simulated cloud top up to this stage seems to verify Fujita's description of jumping cirrus. The average horizontal speed is about 10 m s⁻¹, also quite substantial to deserve the adjective "jump."

The right panel in Fig. 7 shows the receding stage of the jumping cirrus. During this stage, the cirrus gradually retreats and becomes a long stretched plume that is roughly parallel to, but above, the storm anvil and should eventually evaporate to moisten the stratosphere.

Note that all the different motions mentioned above are relative to the motion of the storm. In our simulations, this storm is moving to the east with a speed roughly the same as the midlevel winds which vary with time as the storm develops. Hence the seemingly upstream-ward jump is only relative to the storm itself and not necessary indicating upstream motion relative to the earth.

4.1 CloudSat Observational Evidence of Jumping Cirrus

All the observational data mentioned above are taken either from aircraft, or from geostationary and polar orbiting satellite images using conventional horizontal scan imagers.
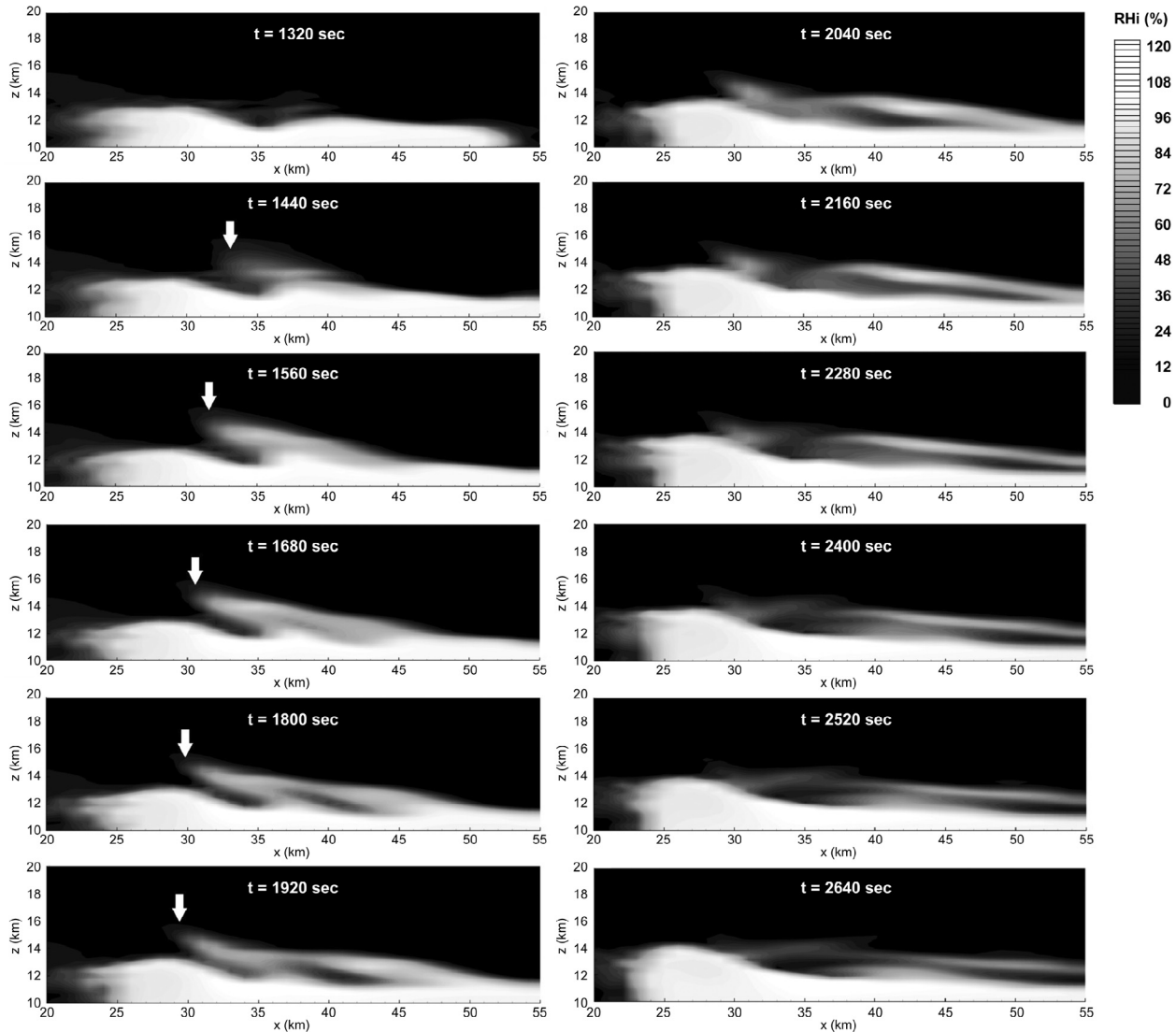
Fig. 7. Snapshots of the RHi profiles in the central east-west cross-section of the simulated storm from t = 1320 to 2640 s. Note each image is windowed to 20 - 55 km in the x-direction and 10 - 20 km in z-direction. The "front" of the jumping cirrus is indicated by the white arrow. The figure is based on a simulation of the CCOPE supercell using a resolution of $1 \times 1 \times 0.2$ km^3 (from Wang 2004).
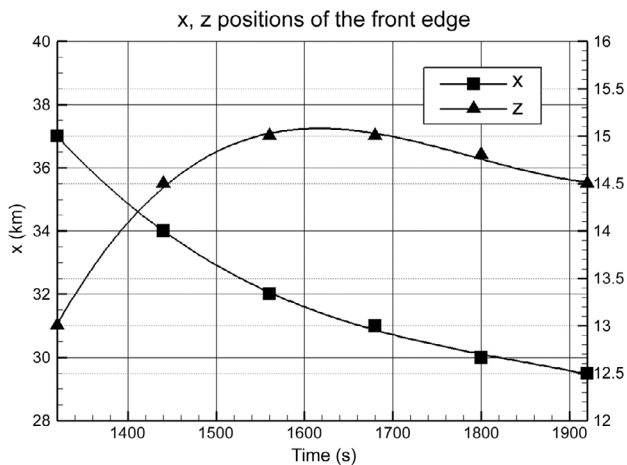

Fig. 8. The x- and z-position of the cloud front of the jumping cirrus as a function of time as shown in Fig. 7.

These traditional satellite images do not resolve the vertical structure of clouds as they generally lack vertical resolution, although some qualitative information can be obtained by examining certain features such as the shadows and infrared brightness temperature. It will be difficult to determine whether an observed above-anvil plume is the overshooting plume or jumping cirrus based on these images alone.

The more recent CloudSat, on the other hand, uses high frequency (94 GHz) cloud profiling radar to perform vertical scan and is able to obtain direct vertical cross-sections of clouds that lie on its path (see http://cloudsat.atmos.colostate.edu/instrument), but it does not provide horizontally scanned cloud images. The CloudSat profiles can be compared to data from other meteorological satellites or instruments, either geostationary or polar orbiting, and then the two types of images can be used complementarily to obtain both

horizontal and vertical information of the cloud. Among these the Aqua/MODIS plays a crucial role, as it covers the same area of interest preceding the CloudSat satellite by one to two minutes only. One of us (ZC) has recently identified a case of jumping cirrus from such a complementary pair of images as shown in Fig. 9.

Figure 9a shows the CloudSat cross-section of a convective cloud system which occurred on 14 November 2009
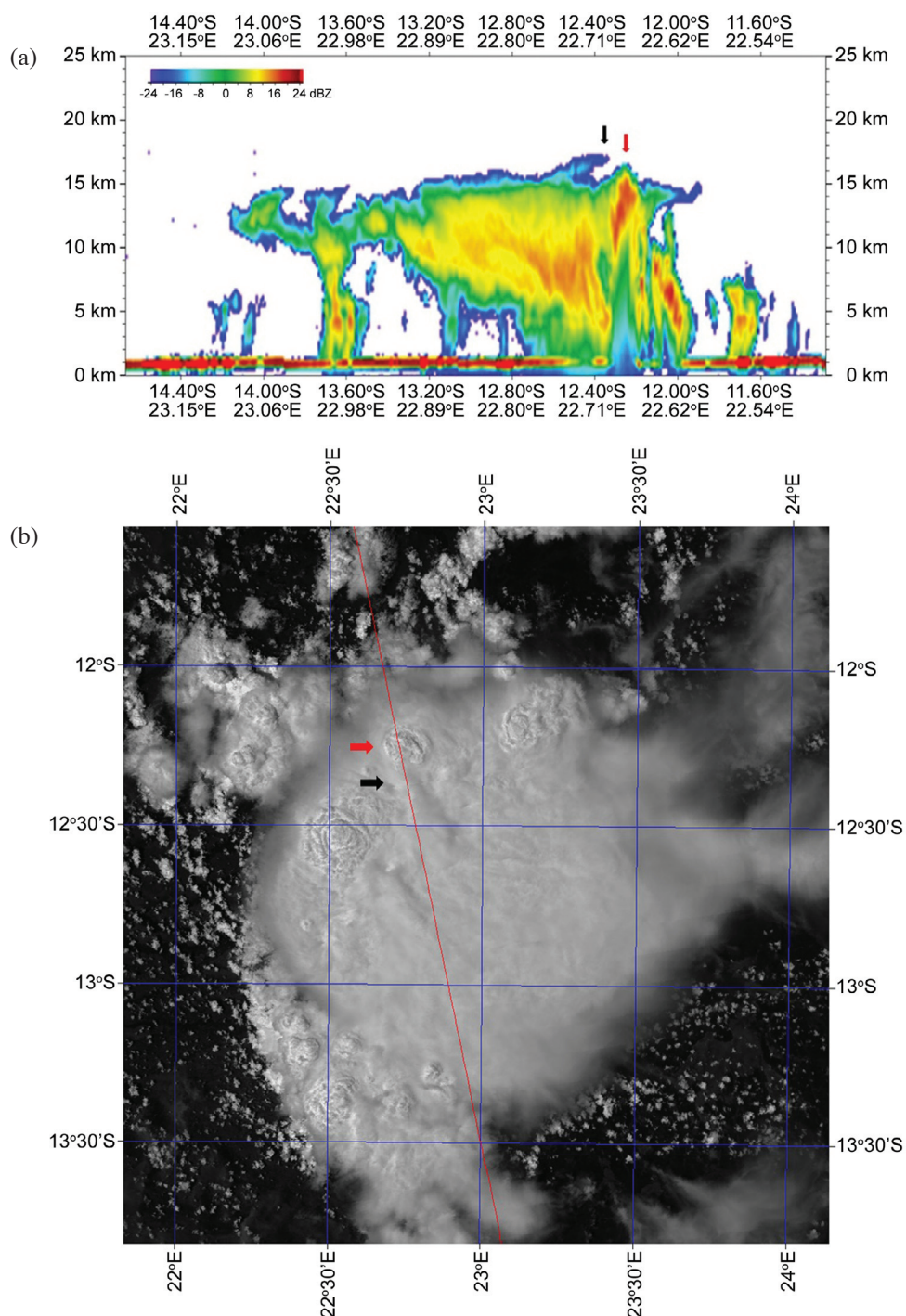

Fig. 9. (a) CloudSat image at 1220 UTC 14 November 2009, showing a jumping cirrus occurrence (black arrow) at the top of a deep convective storm system over eastern Angola in Central Africa (in the Southern Hemisphere). The overshooting top of the storm is indicated by the red arrow. The jumping cirrus was downwind of the overshooting top (data source: NASA/CloudSat). (b) MODIS band 1 image at 1220 UTC 14 November 2009, showing the storm system corresponding to the one with the jumping cirrus in (a). The approximate positions of the jumping cirrus and the overshooting top are indicated by the black and red arrows, respectively. The red line represents the track of CloudSat from south to north (data source: NOAA).

and the feature indicated by the arrow has the characteristics of jumping cirrus. It is located downwind of, but points toward, the overshooting top. It also reaches somewhat above 17 km, slightly higher than the overshooting top.

Figure 9b shows the corresponding MODIS image taken at about the same time. The red line in this figure represents the track of the CloudSat (from south to north). We see that the jumping cirrus in Fig. 9a corresponds to the plume-like structure that seems to be related to the overshooting top to its northeast. The plume casts a shadow on the anvil below. However, it is impossible to identify the plume as a jumping cirrus by the MODIS image alone. For example, there is another plume to the SW of the above jumping cirrus. It is associated with the overshooting top of another storm and it casts a shadow also, but we don't know whether that it is a jumping cirrus or not although it is likely. Such feature is observed frequently in satellite storm images but further studies will be needed to estimate the global frequency.

4.2 Ground-Based Observations of Jumping Cirrus

Aside from satellite observations, Wang et al. (2009) also provided two ground-based observational evidence, both are available in the form of a movie. Selected frames from these movies are given below.

Figure 10 shows a frame from a movie of a storm taken by a north-looking webcam installed on top of the Institute of Atmospheric Physics Building, Federal Institute of Technology (ETH), Zurich, Switzerland, on 5 August 2003 at around 1500 local time. The storm system developed in the general area of south Germany and was clearly a multicellular system judging from the movie. The upper level wind was generally westerly so that the cells generally tilted to the east. As older cells moved to the east and dissipated, new cells appeared in the west and grew rapidly. As soon as a cell reached a sufficient height, presumably close to the tropopause, a jumping cirrus developed at the cloud top; each looks like that shown in Fig. 10. The jumping cirrus also generally points to the west, i.e., upstream, the same as the model results in Fig. 7. This movie can be downloaded at the following URL: http://windy.aos.wisc.edu/pao/jumping_cirrus_movies.htm (Courtesy of Willi Schmid).

Figure 11 is a snapshot of the RHi 50% isosurface of a WISCDYMM simulated storm using the sounding of Stuttgart, Germany at 1800 UTC on 5 August 2003. Stuttgart is approximately 160 km to the NE of Zurich. The general storm environmental condition appears to be similar to the one seen in the webcam movie although precise correspondence is, of course, not expected. But the general behavior of the simulated storm top jumping cirrus resembles that seen in the movie. The movie and the simulation demonstrate that the jumping cirrus and the ensuing transport of water into the stratosphere are not limited to supercell but can occur in multicell storms as well.

There is another movie showing the jumping cirrus on top of a thunderstorm that occurred in Denver available at the following URL: http://windy.aos.wisc.edu/pao/jumping_cirrus_movies.htm (Courtesy of Walter Lyons). This was taken by a camera on the ground looking up to the thunderstorm system. Because of the view angle, the overshooting top was blocked by the extensive anvil when the storm was passing overhead. Nevertheless, the cirrus clouds moving up and down above the anvil can be clearly seen from the movie.
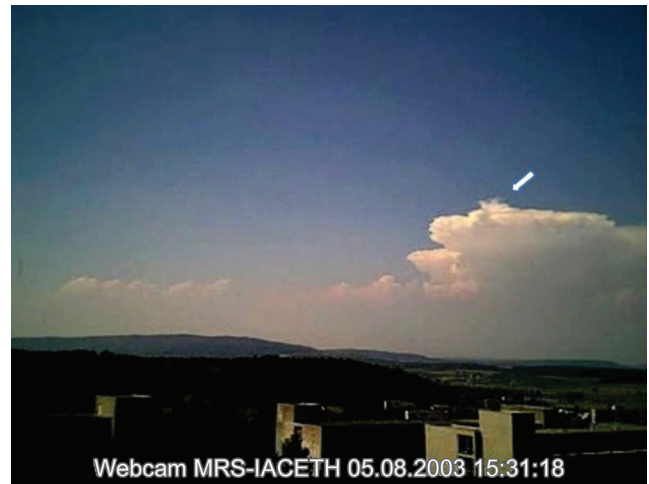

Fig. 10. A frame taken from a movie of a thunderstorm occurred on 5 August 2003 in Bavaria region of Germany, as seen by a webcam mounted on top of the Institute of Atmospheric and Climate Science Building, Federal Institute of Technology (ETH), at Zurich, Switzerland. The jumping cirrus is indicated by the white arrow.
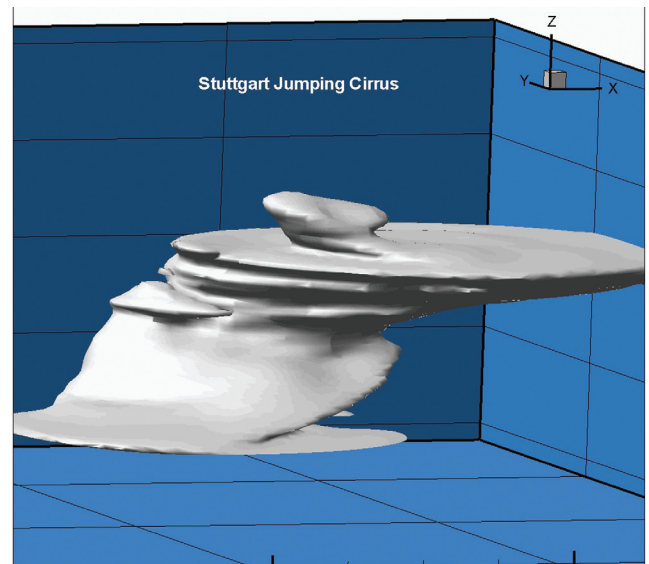

Fig. 11. A snapshot of the simulated storm using sounding from Stuttgart, Germany, 1200 UTC 5 August 2003, showing the jumping cirrus formed at the cloud top.

5. OTHER OBSERVATIONAL EVIDENCE OF INJECTION OF WATER SUBSTANCE INTO THE STRATOSPHERE BY DEEP CONVECTIVE CLOUDS

All the evidence provided above is based on visual observations and is mainly from thunderstorms which occurred in mid-latitudes. Deep convective storms occur in the tropics as well and one would expect that they will also transport water substance through the tropopause into the mid-latitudes stratosphere. However, the cloud top level wind shear is stronger in the mid-latitudes and weaker in the tropics. This makes the identification of the above anvil plumes in the tropics a more difficult task as the elongation of the plume by wind is not as obvious as mid-latitude cases. There are differences between the deep convective storms in the mid-latitudes and the tropics. The tropopause in the tropics is much higher than in the mid-latitudes, and whether or not regular deep convective clouds with relatively weak convective available potential energy can penetrate the tropopause is still debated (see, e.g., Folkins et al. 1999). Since the gravity wave breaking process is related to wind shear also, it is not yet clear at present how the weaker wind shear in the tropical upper troposphere influences the penetrative transport of water substance into the stratosphere. For a more general discussion of deep tropical convection, see Emanuel (1994). For more recent observational discussions of water vapor transport through the tropical tropopause, see Randel et al. (2001, 2006).

Nevertheless, there are already direct samplings of stratospheric air that contains ice particles that are believed to originate from storms in tropical latitudes. For example, Danielsen (1993) observed the presence of a stratospheric anvil during the Stratosphere-Troposphere Exchange Project (STEP) in Darwin, Australia in January - February 1987. More recently, Corti et al. (2008) analyzed the remote sensing aircraft data from the Tropical Convection, Cirrus, and Nitrogen Oxides Experiment (TROCCINOX) in the State of Sao Paulo, Brazil in February 2005 and the Stratosphere-Climate Links with Emphasis on the Upper Troposphere and Lower Stratosphere (SCOUT-O3) experiment in Darwin, Australia, in November/December 2005. They found ice particles in the stratospheric "overworld" [the part of the stratosphere above ~380 K isentropic surface which is thought to be not directly influenced by tropospheric processes. See Hoskins (1991) or Holton et al. (1995)] and concluded that the only possible explanation is that most ice particles are transported by deep convection. Similarly, Khaykin et al. (2008) performed balloon-borne soundings of water vapor, particles and ozone in the lower stratosphere next to mesoscale convective systems during the monsoon season over West Africa in Niamey, Niger, in August 2006, and showed also the presence of ice particles in the lower stratosphere.

Interestingly, these lower latitude observations tend to portray the deep convective clouds as the moisturizer of the stratosphere whereas conventionally they are thought to play the role of desiccator. Because tropical deep convective clouds are thought to reach very high in the troposphere, the cloud top temperatures are very cold and water vapor should almost completely convert into ice crystals and fall out, leaving very dry air to continue its journey into the stratosphere. This is the so-called "freeze dry" mechanism and is often cited as the reason why the stratosphere is so dry with only 3 - 6 ppm of water vapor (see, for example, Brewer 1949; Kley et al. 1979; Newell and Gould-Stewart 1981). This somewhat confusing status of the role played by the deep tropical convection is apparently not completely resolved at present and more research is needed to resolve the issue.

Finally, recent observations of the water isotope HDO in the UTLS also support the deep convective transport cross the tropopause. HDO is more susceptible to condensation than H2O because of the heavier deuterium in the molecule. If water vapor in the troposphere is carried upward by slow ascend, it is expected that the HDO/H_2O ratio should be very small in the UTLS because most of the HDO would have condensed and precipitated out. Yet both satellite data (Moyer et al. 1996; Kuang et al. 2003) and aircraft observations (Hanisco et al. 2007) show that the UTLS HDO/H_2O ratio is much higher than can be explained by the slow ascend scenario. On the other hand, if the tropospheric water is transported by rapid convection to deep convective storms, then the water vapor can be transported so rapidly by the strong updrafts in these storms that HDO either wouldn't have time to condense, or if it does condense, the resulting condensed water (mostly in ice form) can be injected directly into the UTLS and eventually evaporate to give the high HDO/H_2O ratio. The overshooting plumes and jumping cirrus outlined in the previous sections can serve exactly such a role to inject high HDO content water into the lower stratosphere. The aircraft observations of ice crystals in the lower stratosphere described in the first paragraph of this section convincingly testify the existence of these processes.

6. IMPLICATIONS OF THE DEEP CONVECTIVE TRANSPORT OF WATER INTO THE STRATOSPHERE

The indication that deep convective storms are capable of transporting water substance from the troposphere into the stratosphere has important implications to many aspects of atmospheric science. This will be described below.

First of all, it complicates the simple view of conventional general circulation of the atmosphere. It is well known by now that the 3-cell general circulation model (Hadley, Ferrel and Polar) is an Eulerian interpretation while the Brewer-Dobson circulation is more appropriate for the material circulation (see, e.g., Plumb and Eluszkie-

wicz 1999). A schematic view of this type of circulation that includes the stratosphere is provided by Holton et al. (1995). It explains how air masses, including water vapor, can be transported globally.

The water vapor would be transported from the tropical boundary layer by deep convective clouds in the tropics to the upper troposphere and penetrate through the tropopause into the stratosphere. Once in the stratosphere, the vapor will be pumped towards mid- and high latitudes via the "extratropical pump" mechanism induced by Rossby wave breaking in the mid-latitude stratosphere. Then somewhere in the mid-latitudes the vapor will be brought down to the troposphere by the downward circulation via certain mixing processes and complete the cycle.

The above point of view is based on the mean circulation. But, as Danielsen (1982) argued, the mean flow point of view may miss the real physical process because the mean flow circulations may just be small residuals of the much stronger convective circulations that are doing the physical transport between the troposphere and stratosphere. The finding of the cross-tropopause transport of water substance by mid-latitude deep convective storms reported here confirms this argument. Apparently, the true process of global material transport in the atmosphere is more complicated than can be described by the mean flow scheme. Thus the mid-latitudes can also be a source region of water substance and not just play the role of a sink.

The simple global zonal mean circulation is made further complicated by the finding that there appears to exist a barrier at z ~14 km in the tropical troposphere that makes the vertical transport of matters difficult (see, e.g., Folkins et al. 1999). Highwood and Hoskins (1998) also reported that the top of tropical deep convective clouds rarely exceed 14 km. If this is indeed the case, then how water vapor can be transported through the tropical tropopause as is required by the mean circulation becomes unclear. The layer of the tropical troposphere between 14 and 17 km is now usually called the tropical tropopause layer (TTL) (see, e.g., a review by Fueglistaler et al. 2009). Obviously, there is an urgent need to understand the tropical deep convective cloud behavior near TTL to resolve these difficulties.

Second, as mentioned before, the water that is transported into the stratosphere by deep convective storms may have a residence time longer than a year and hence has the potential of playing a climatic forcing role. Although the amount of water so injected is small, its climatic impact might be large due to significant radiative interaction between water vapor and infrared radiation in the stratosphere (Solomon et al. 2010). If the stratospheric water vapor concentration changes with time, then this unsteadiness may cast a strong influence on the climate system. It is well-known that stratospheric water vapor concentration has been changing over the last few decades (see, e.g., Oltmans et al. 2000; Rosenlof et al. 2001). Solomon et al. (2010)

suggested that the omission of the effect of stratospheric water vapor may be responsible for the over-prediction of warming in the last few years in many climate models. This means that we need to understand more clearly how water gets into the stratosphere before we can make more accurate climate prediction using numerical climate models. Some discussion on the larger scale convective transport of water vapor into the UTLS has been given by Dessler and Sherwood (2004) and Dessler (2009).

Third, if the deep convective storms can transport water substance into the stratosphere, they can also transport other chemical species (trace gases and aerosols) as well via the same mechanism. Water vapor is subject to the freeze-dry mechanism at the low tropopause temperature but many other species do not behave similarly and they may be injected into the stratosphere efficiently by this convective transport. If this is the case, then their impact on the atmosphere needs to be carefully considered. This is especially true for assessing the impact of many anthropogenic chemicals that can be transported by deep convective systems to upper troposphere and lower stratosphere (UTLS). Other modeling studies (e.g., Mullendore et al. 2005; Luderer et al. 2006; Trentmann et al. 2006) of the penetrative transport of other tracers indicate that this indeed happens. The emission of these chemicals varies from region to region - industrially advanced countries emit man-made chemicals that are often of a different nature from those emitted by developing countries. How deep convective systems transport these chemicals up to the UTLS and their impact on the global atmospheric system deserves to be studied closely.

7. SUMMARY AND OUTLOOK

Observational evidence is summarized to show that mid-latitude deep convective storms inject water substance including water vapor and ice particles through the tropopause into the stratosphere. Model studies indicate that this is achieved via the storm top gravity wave breaking and turbulent mixing induced instability. Because of its potential climate forcing, it is necessary to understand this transport process more quantitatively. So far the model studies only provide qualitative conclusions about the possible mechanisms but no adequate quantitative assessment of the importance of this transport has been made due to the lack of comparison between model results and observational data. It will be desirable to develop global observational (presumably satellite) techniques that can estimate more quantitatively this transport. More refined numerical models, both storm and larger scales, are also needed to understand the broader impact of the transport.

REFERENCES

Brasseur, G. P., J. J. Orlando, and G. S. Tyndall, 1999: Atmospheric Chemistry and Global Change. Oxford University Press, 654 pp.

Brewer, A. W., 1949: Evidence for a world circulation provided by the measurements of helium and water vapour distribution in the stratosphere. *Q. J. R. Meteorol. Soc.*, **75**, 351-363, doi: 10.1002/qj.49707532603. [Link]

Corti, T., B. P. Luo, M. de Reus, D. Brunner, F. Cairo, M. J. Mahoney, G. Martucci, R. Matthey, V. Mitev, F. H. dos Santos, C. Schiller, G. Shur, N. M. Sitnikov, N. Spelten, H. J. Vössing, S. Borrmann, and T. Peter, 2008: Unprecedented evidence for deep convection hydrating the tropical stratosphere. *Geophys. Res. Lett.*, **35**, L10810, doi: 10.1029/2008GL033641. [Link]

Danielsen, E. F., 1982: A dehydration mechanism for the stratosphere. *Geophys. Res. Lett.*, **9**, 605-608, doi: 10. 1029/GL009i006p00605. [Link]

Danielsen, E. F., 1993: In situ evidence of rapid, vertical, irreversible transport of lower tropospheric air into the lower tropical stratosphere by convective cloud turrets and by larger-scale upwelling in tropical cyclones. *J. Geophys. Res.*, **98**, 8665-8681, doi: 10.1029/92JD029 54. [Link]

Dessler, A. E., 2009: Clouds and water vapor in the Northern Hemisphere summertime stratosphere. *J. Geophys. Res.*, **114**, D00H09, doi: 10.1029/2009JD012075. [Link]

Dessler, A. E. and S. C. Sherwood, 2004: Effect of convection on the summertime extratropical lower stratosphere. *J. Geophys. Res.*, **109**, D23301, doi: 10.1029/20 04JD005209. [Link]

Emanuel, K. A., 1994: Atmospheric Convection. Oxford University Press, 592 pp.

Folkins, I., M. Loewenstein, J. Podolske, S. J. Oltmans, and M. Proffitt, 1999: A barrier to vertical mixing at 14 km in the tropics: Evidence from ozonesondes and aircraft measurements. *J. Geophys. Res.*, **104**, 22095-22102, doi: 10.1029/1999JD900404. [Link]

Forster, P. M. de F. and K. P. Shine, 2002: Assessing the climate impact of trends in stratospheric water vapor. *Geophys. Res. Lett.*, **29**, 1086, doi: 10.1029/2001GL0 13909. [Link]

Fritz, S. and I. Laszlo, 1993: Detection of water vapor in

the stratosphere over very high clouds in the tropics. *J. Geophys. Res.*, **98**, 22959-22967, doi: 10.1029/93JD01 617. [Link]

Fueglistaler, S., A. E. Dessler, T. J. Dunkerton, I. Folkins, Q. Fu, and P. W. Mote, 2009: Tropical tropopause layer. *Rev. Geophys.*, **47**, RG1004, 1-31, doi: 10.1029/ 2008RG000267. [Link]

Fujita, T. T., 1982: Principle of stereographic height computations and their application to stratospheric cirrus over severe thunderstorms. *J. Meteorol. Soc. Jpn.*, **60**, 355-368.

Fujita, T. T., 1989: The Teton-Yellowstone tornado of 21 July 1987. *Mon. Weather Rev.*, **117**, 1913-1940, doi: 10.1175/1520-0493(1989)117<1913:TTYTOJ>2.0.C O;2. [Link]

Hanisco, T. F., E. J. Moyer, E. M. Weinstock, J. M. St. Clair, D. S. Sayres, J. B. Smith, R. Lockwood, J. G. Anderson, A. E. Dessler, F. N. Keutsch, J. R. Spackman, W. G. Read, and T. P. Bui, 2007: Observations of deep convective influence on stratospheric water vapor and its isotopic composition. *Geophys. Res. Lett.*, **34**, L04814, doi: 10.1029/2006GL027899. [Link]

Hassim, M. E. E. and T. P. Lane, 2010: A model study on the influence of overshooting convection on TTL water vapour. *Atmos. Chem. Phys.*, **10**, 9833-9849, doi: 10. 5194/acp-10-9833-2010. [Link]

Highwood, E. J. and B. J. Hoskins, 1998: The tropical tropopause. *Q. J. R. Meteorol. Soc.*, **124**, 1579-1604, doi: 10.1002/qj.49712454911. [Link]

Holton, J. R., P. H. Haynes, M. E. McIntyre, A. R. Douglass, R. B. Rood, and L. Pfister, 1995: Stratosphere-troposphere exchange. *Rev. Geophys.*, **33**, 403-439, doi: 10.1029/95RG02097. [Link]

Hoskins, B. J., 1991: Towards a PV-θ view of the general circulation. *Tellus A*, **43**, 27-35, doi: 10.1034/j.1600-0 870.1991.t01-3-00005.x. [Link]

Johnson, D. E., P. K. Wang, and J. M. Straka, 1993: Numerical simulations of the 2 August 1981 CCOPE supercell storm with and without ice microphysics. *J. Appl. Meteorol.*, **32**, 745-759, doi: 10.1175/1520-0450(1993) 032<0745:NSOTAC>2.0.CO;2. [Link]

Johnson, D. E., P. K. Wang, and J. M. Straka, 1994: A study of microphysical processes in the 2 August 1981 CCOPE supercell storm. *Atmos. Res.*, **33**, 93-123, doi: 10.1016/0169-8095(94)90015-9. [Link]

Khaykin, S., J. P. Pommereau, L. Korshunov, V. Yushkov, J. Nielsen, N. Larsen, T. Christensen, A. Garnier, A. Lukyanov, and E. William, 2008: Hydration of the lower stratosphere by ice crystal geysers over land convective systems. *Atmos. Chem. Phys. Discuss.*, **8**, 15463-15490, doi: 10.5194/acpd-8-15463-2008. [Link]

Kley, D., E. J. Stone, W. R. Henderson, J. W. Drummond, W. J. Harrop, A. L. Schmeltekopf, T. L. Thompson, and R. H. Winkler, 1979: *In situ* measurements of the mix-

ing ratio of water vapor in the stratosphere. *J. Atmos. Sci.*, **36**, 2513-2524, doi: 10.1175/1520-0469(1979)036 <2513:SMOTMR>2.0.CO;2. [Link]

Knight, C. A., 1982: The Cooperative Convective Precipitation Experiment (CCOPE), 18 May-7 August 1981. *Bull. Amer. Meteorol. Soc.*, **63**, 386-398, doi: 10.1175/ 1520-0477(1982)063<0386:TCCPEM>2.0.CO;2. [Link]

Kuang, Z., G. C. Toon, P. O. Wennberg, and Y. L. Yung, 2003: Measured HDO/H_2O ratios across the tropical tropopause. *Geophys. Res. Lett.*, **30**, 1372, doi: 10.1029/ 2003GL017023. [Link]

Levizzani, V. and M. Setvák, 1996: Multispectral, high resolution satellite observations of plumes on top of convective storms. *J. Atmos. Sci.*, **53**, 361-369, doi: 10.11 75/1520-0469(1996)053<0361:MHRSOO>2.0.CO;2. [Link]

Lin, H., P. K. Wang, and R. E. Schlesinger, 2005: Three-dimensional nonhydrostatic simulations of summer thunderstorms in the humid subtropics versus High Plains. *Atmos. Res.*, **78**, 103-145, doi: 10.1016/j.atmosres.200 5.03.005. [Link]

Liou, K. N., 1992: Radiation and Cloud Processes in the Atmosphere: Theory, Observation, and Modeling. Oxford University Press, New York, 504 pp.

Luderer, G., J. Trentmann, T. Winterrath, C. Textor, M. Herzog, H. F. Graf, and M. O. Andreae, 2006: Modeling of biomass smoke injection into the lower stratosphere by a large forest fire (Part II): Sensitivity studies. *Atmos. Chem. Phys.*, **6**, 5261-5277, doi: 10.5194/acp-6-5261-2006. [Link]

Moyer, E. J., F. W. Irion, Y. L. Yung, and M. R. Gunson, 1996: ATMOS stratospheric deuterated water and implications for troposphere-stratosphere transport. *Geophys. Res. Lett.*, **23**, 2385-2388, doi: 10.1029/96GL0 1489. [Link]

Mullendore, G. L., D. R. Durran, and J. R. Holton, 2005: Cross-tropopause tracer transport in midlatitude convection. *J. Geophys. Res.*, **110**, D06113, doi: 10.1029/ 2004JD005059. [Link]

Myhre, G., J. S. Nilsen, L. Gulstad, K. P. Shine, B. Rognerud, and I. S. A. Isaksen, 2007: Radiative forcing due to stratospheric water vapour from CH_4 oxidation. *Geophys. Res. Lett.*, **34**, L01807, doi: 10.1029/2006GL 027472. [Link]

Newell, R. E. and S. Gould-Stewart, 1981: A stratospheric fountain? *J. Atmos. Sci.*, **38**, 2789-2796, doi: 10.1175/ 1520-0469(1981)038<2789:ASF>2.0.CO;2. [Link]

Oltmans, S. J., H. Völmel, D. J. Hofmann, K. H. Rosenlof, and D. Kley, 2000: The increase in stratospheric water vapor from balloonborne, frostpoint hygrometer measurements at Washington, D. C., and Boulder, Colorado. *Geophys. Res. Lett.*, **27**, 3453-3456, doi: 10.1029/ 2000GL012133. [Link]

Pan, L., S. Soloman, W. Randel, J.-F. Lamarque, P. Hess, J. Gille, E. W. Chiou, and M. P. McCormick, 1997: Hemispheric asymmetries and seasonal variations of the lowermost stratospheric water vapor and ozone derived from SAGE II data. *J. Geophys. Res.*, **102**, 28177 -28184, doi: 10.1029/97JD02778. [Link]

Pan, L. L., E. J. Hintsa, E. M. Stone, E. M. Weinstock, and W. J. Randel, 2000: The seasonal cycle of water vapor and saturation vapor mixing ratio in the extratropical lowermost stratosphere. *J. Geophys. Res.*, **105**, 26519-26530, doi: 10.1029/2000JD900401. [Link]

Plumb, R. A. and J. Eluszkiewicz, 1999: The Brewer-Dobson circulation: Dynamics of the tropical upwelling. *J. Atmos. Sci.*, **56**, 868-890, doi: 10.1175/1520-0469(19 99)056<0868:TBDCDO>2.0.CO;2. [Link]

Randel, W. J., F. Wu, A. Gettelman, J. M. Russell III, J. M. Zawodny, and S. J. Oltmans, 2001: Seasonal variation of water vapor in the lower stratosphere observed in Halogen Occultation Experiment data. *J. Geophys. Res.*, **106**, 14313-14325, doi: 10.1029/2001JD900048. [Link]

Randel, W. J., F. Wu, H. Vömel, G. E. Nedoluha, and P. Forster, 2006: Decreases in stratospheric water vapor after 2001: Links to changes in the tropical tropopause and the Brewer-Dobson circulation. *J. Geophys. Res.*, **111**, D12312, doi: 10.1029/2005JD006744. [Link]

Roach, W. T., 1967: On the nature of the summit areas of severe storms in Oklahoma. *Q. J. R. Meteorol. Soc.*, **93**, 318-336, doi: 10.1002/qj.49709339704. [Link]

Rosenlof, K. H., 2003: How water enters the stratosphere. *Science*, **302**, 1691-1692, doi: 10.1126/science.10927 03. [Link]

Rosenlof, K. H., S. J. Oltmans, D. Kley, J. M. Russell III, E. W. Chiou, W. P. Chu, D. G. Johnson, K. K. Kelly, H. A. Michelsen, G. E. Nedoluha, E. E. Remsberg, G. C. Toon, M. P. McCormick, 2001: Stratospheric water vapor increases over the past half-century. *Geophys. Res. Lett.*, **28**, 1195-1198, doi: 10.1029/2000GL012502. [Link]

Setvák, M. and C. A. Doswell, 1991: The AVHRR channel 3 cloud top reflectivity of convective storms. *Mon. Weather Rev.*, **119**, 841-847, doi: 10.1175/1520-0493 (1991)119<0841:TACCTR>2.0.CO;2. [Link]

Setvák, M., D. T. Lindsey, R. M. Rabin, P. K. Wang, A. Demeterová, 2008: Indication of water vapor transport into the lower stratosphere above midlatitude convective storms: Meteosat Second Generation satellite observations and radiative transfer model simulations. *Atmos. Res.*, **89**, 170-180, doi: 10.1016/j.atmosres.2007. 11.031. [Link]

Shindell, D. T., 2001: Climate and ozone response to increased stratospheric water vapor. *Geophys. Res. Lett.*, **28**, 1551-1554, doi: 10.1029/1999GL011197. [Link]

Solomon, S., 1999: Stratospheric ozone depletion: A review

of concepts and history. *Rev. Geophys.*, **37**, 275-316, doi: 10.1029/1999RG900008. [Link]

Solomon, S., D. Qin, M. Manning, R. B. Alley, T. Berntsen, N. L. Bindoff, Z. Chen, A. Chidthaisong, J. M. Gregory, G. C. Hegerl, M. Heimann, B. Hewitson, B. J. Hoskins, F. Joos, J. Jouzel, V. Kattsov, U. Lohmann, T. Matsuno, M. Molina, N. Nicholls, J. Overpeck, G. Raga, V. Ramaswamy, J. Ren, M. Rusticucci, R. Somerville, T. F. Stocker, P. Whetton, R. A. Wood, and D. Wratt, 2007: Technical summary. In: Solomon, S., D. Qin, M. Manning, Z. Chen, M. Marquis, K. B. Averyt, M. Tignor, and H. L. Miller (Eds.), Climate Change 2007: The Physical Science Basis, Contribution of Working Group I to the Fourth Assessment Report of the Intergovernmental Panel on Climate Change, Cambridge University Press, Cambridge, United Kingdom and New York, NY, USA.

Solomon, S., K. H. Rosenlof, R. W. Portmann, J. S. Daniel, S. M. Davis, T. J. Sanford, and G. K. Plattner, 2010: Contributions of stratospheric water vapor to decadal changes in the rate of global warming. *Science*, **327**, 1219-1223, doi: 10.1126/science.1182488. [Link]

Straka, J. M., 1989: Hail growth in a highly glaciated central High Plains multi-cellular hailstorm. Ph.D. Dissertation, Department of Meteorology, University of Wisconsin-Madison, 413 pp.

Trentmann, J., G. Luderer, T. Winterrath, M. D. Fromm, R. Servranckx, C. Textor, M. Herzog, H. F. Graf, and M. O. Andreae, 2006: Modeling of biomass smoke injection into the lower stratosphere by a large forest fire (Part I): Reference simulation. *Atmos. Chem. Phys.*, **6**, 5247-5260, doi: 10.5194/acp-6-5247-2006. [Link]

Wade, C. G., 1982: A preliminary study of an intense thunderstorm which move across the CCOPE research network in southeastern Montana. Paper presented at Ninth Conference on Weather Forecasting and Analysis, Am. Meteorol. Soc., Seattle, Wash.

Wang, P. K., 2003: Moisture plumes above thunderstorm anvils and their contributions to cross tropopause transport of water vapor in midlatitudes. *J. Geophys. Res.*, **108**, 4194, doi: 10.1029/2002JD002581. [Link]

Wang, P. K., 2004: A cloud model interpretation of jumping cirrus above storm top. *Geophys. Res. Lett.*, **31**, L18106, doi: 10.1029/2004GL020787. [Link]

Wang, P. K., 2007: The Thermodynamic structure atop a penetrating convective thunderstorm. *Atmos. Res.*, **83**, 254-262, doi: 10.1016/j.atmosres.2005.08.010. [Link]

Wang, P. K., M. Setvák, W. Lyons, W. Schmid, and H. M. Lin, 2009: Further evidences of deep convective vertical transport of water vapor through the tropopause. *Atmos. Res.* **94**, 400-408, doi: 10.1016/j.atmosres.2009.06.018. [Link]